Combining multiphoton and CARS microscopy for skin imaging

H. G. Breunig[a,b,*], M. Weinigel[a], M. Kellner-Höfer[a], R. Bückle[a], M. E. Darvin[c], J. Lademann[c], K. König[a,b]

[a]JenLab GmbH, Schillerstr 1, 07745 Jena, Germany and Science Park 2, Campus D1.2, 66123 Saarbrücken, Germany

[b]Saarland University, Faculty of Mechatronics and Physics, Department of Biophotonics and Laser Technology, Campus A5.1, 66123 Saarbrücken, Germany

[c]Charité-Universitätsmedizin Berlin, Department of Dermatology and Allergology, Center of Experimental and Cutaneous Physiology (CCP), 10117 Berlin, Germany

ABSTRACT

Microscopic imaging based on multiphoton fluorescence, second harmonic generation (SHG) and coherent anti-Stokes Raman scattering (CARS) imaging has been realized in one common platform which is appropriate for use in hospitals. The different optical modalities non-invasively provide in vivo images from human skin with subcellular resolution, at different depths based on endogenous fluorescent, SHG-active molecules as well as non-fluorescent molecules with vibrational resonances at 2845 cm^{-1}, in particular lipids. An overview of the system employing a Ti:sapphire laser and photonic crystal fiber to generate the excitation light as well as several imaging examples are presented.

Keywords: CARS, CARS imaging, non-linear microscopy, skin imaging, multiphoton imaging, lipids.

1. INTRODUCTION

Biomedical in-vivo imaging of tissue with subcellular resolution, high sensitivity and chemical discrimination has provided previously unavailable insight into biomedical system[1,2]. High resolution non-invasive imaging can be achieved by optical techniques. By combining different optical techniques different signal sources can be exploited to gain mutually completing information. We describe a system which combines the optical techniques two-photon fluorescence (TPF), second harmonic generation and coherent anti Stokes Raman scattering (CARS) for clinical imaging. While similar versatile laboratory-used imaging setups have been developed already several years ago[3] there is currently still only one system (by JenLab GmbH with different variants) appropriate and certified for clinical use in hospitals[4-6].

In vivo multiphoton microscopy on human skin is clinically used for early skin cancer diagnostics, skin age determination, to monitor penetration of particles into the skin as well as effects of drugs, and cosmetic compounds[7,8]. Non-invasive subcellular resolution imaging is achieved based on endogenous skin fluorophores and second harmonic generating (SHG) compounds like collagen structures[9]. CARS microscopy can additionally provide access to non-fluorescent but Raman-active molecules, in particular lipids[3,10]. With the strong and distinct CARS signals the drawbacks of spontaneous Raman and infrared (IR) spectroscopy which either lack high sensitivity (which is necessary for fast scanning-laser microscopy[11]) or high resolution, respectively, can be overcome. The nonlinear nature of the CARS process provides also intrinsic 3-D sectioning. CARS signals are generated in case the difference frequency $\Omega = \omega_p - \omega_s$ of pump and Stokes photons with frequencies ω_p and ω_S, respectively, matches the frequency of a Raman active molecular vibration[10]. Different CARS schemes mostly employing ps or fs (or a combination) pulses have been developed[12]. For clinical CARS imaging so far a Ti:sapphire laser in combination with an optical parametric oscillator and a Ti:sapphire laser in combination with a photonic crystal fiber (PCF) which was used to spectrally broaden a part of the laser output have been realized.

*breunig@.jenlab.de; phone ++49-3641-470 501; fax ++49- 3641-470 543; www.jenlab.de

Multiphoton Microscopy in the Biomedical Sciences XIII, edited by Ammasi Periasamy, Karsten König, Peter T. C. So, Proc. of SPIE Vol. 8588, 85880N · © 2013 SPIE · CCC code: 1605-7422/13/$18 · doi: 10.1117/12.2001985

We review here properties of the latter setup and discuss imaging examples. CARS imaging is performed Ω= 2845 cm^{-1}, which correspond to energy of the CH_2 stretch vibration. A strong signal level at 2845 cm^{-1} is often interpreted as a result of lipids. However, in skin and tissue also protein structures such as keratin and collagen fibers can cause considerable signals at this frequency[13,14].

2. MATERIAL AND METHODS

The measurement setup is similar to the one described in Ref. 6. Briefly, the CE-certified clinical multiphoton tomograph DermaInspect (JenLab GmbH) for microscopic in vivo skin investigation was extended by adding CARS-imaging capability[7]. The DermaInspect enables laser-scanning multiphoton imaging in reflection geometry based on the excitation and detection of TPF and SHG signals by near infrared (NIR) fs pulses. The fs pulses are generated by a wavelength-tunable Ti:sapphire oscillator (MaiTai, Spectra-Physics; 80 MHz, 100 fs tuning range 710 nm - 920 nm). The system provides a lateral resolution of about 300 nm and an axial resolution of about 1 µm - 2 µm [7]. Images typically consist of 512 x 512 pixels and cover a maximum region of 350 x 350 μm^2. Detection of endogenous fluorophores like keratin, NAD(P)H, melanin, collagen, elastin, flavin adenine dinucleotide (FAD) and others as well as the detection of externally applied fluorescent labels is possible[7,15].

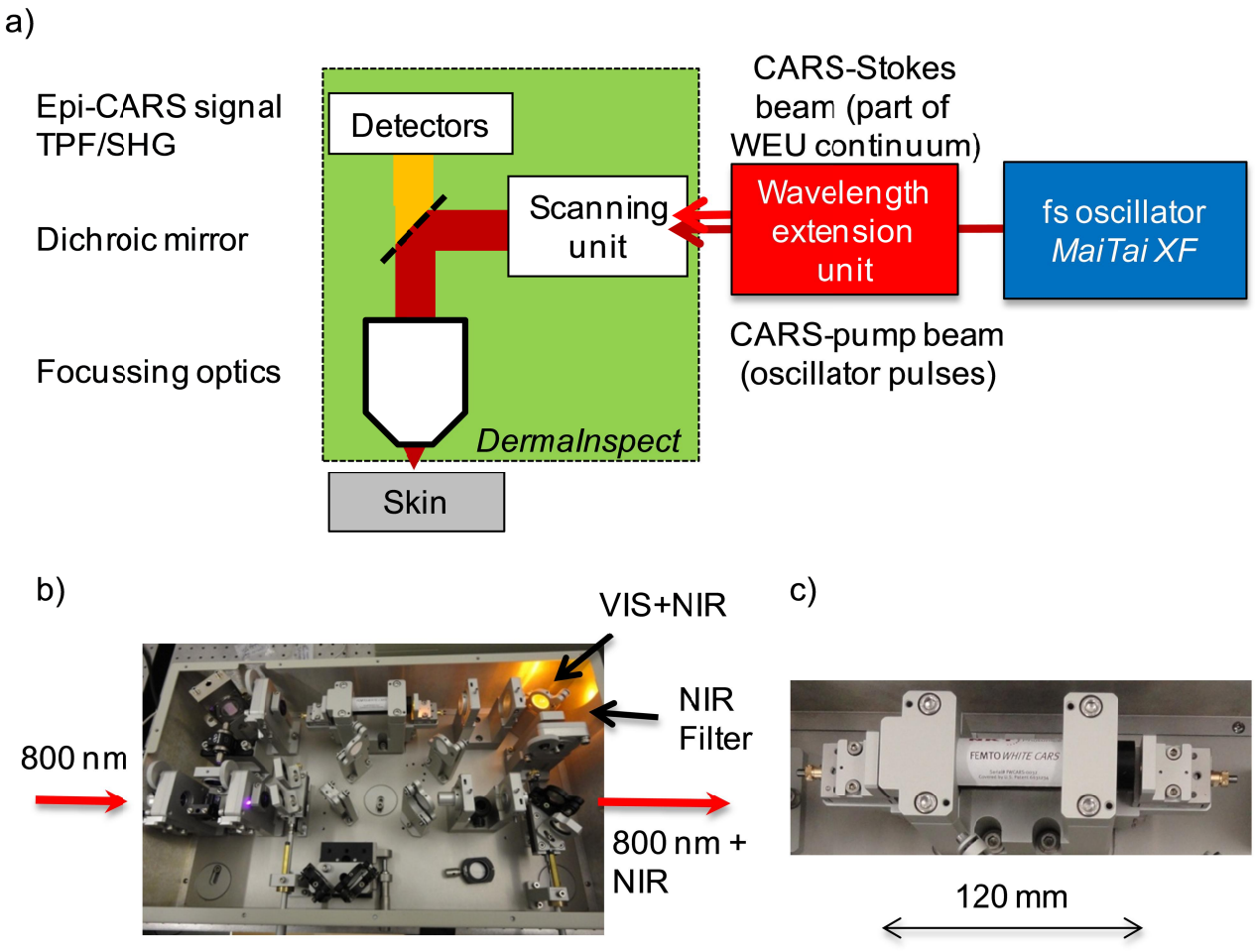

Fig. 1: a) Scheme of the CARS DermaInspect for clinical CARS/TPF/SHG skin imaging. Excitation is provided by a Ti:sapphire laser and a PCF unit which spectrally broadens a part of the laser output. A two-channel detector module enables simultaneous detection of fluorescence and CARS signals. b) View inside the wavelength extension unit which generates an additional NIR beam by splitting and spectrally broadening a part of the incoming 800-nm pulses. A suitable spectral part of the broadened pulses is separated by a filter and used as CARS-Stokes pulses. c) PCF module used to spectrally broaden a part of the of the 800-nm pulses.

The CARS add-on consists of a "wavelength extension unit" (WEU)[16] (Newport-Spectra Physics) which includes a PCF (FemtoWhite CARS, NKT Photonics) module in combination with suitable optics and detectors for CARS imaging. The whole CARS DermaInspect has by itself received a CE certification after evaluation by a certified body as a clinical system. To avoid skin damages by the laser light the total excitation power incident on the skin is kept below 50 mW [17]. For the measurements reported here, the center wavelength of the fs oscillator was usually set to 800 nm. The oscillator pulses were split inside the WEU into two parts, i.e. a two-beam setup was employed. One beam with a mean power of 500 mW was focused into the PCF of the WEU (Fig. 1 b). These pulses were spectrally broadened by self-phase modulation and other non-linear effects inside the fiber (Fig. 1 c)[16]. Spectra of the fs pulses before with and without broadening by the PCF are shown in Fig. 2 a). To excite the CH_2 vibration at 2845 cm^{-1} with 800-nm-pump pulses requires CARS-Stokes pulses at 1035 nm and generates CARS signals at 652 nm. Therefore, a spectral part of the continuum pulses around 1035 nm was selected by a transmission band-pass filter (Chroma HQ1045-30) and subsequently temporally and spatially overlapped with the 800-nm pulses. The spectra of the excitation beam used for CARS-lipid imaging are shown in Fig. 2 b).

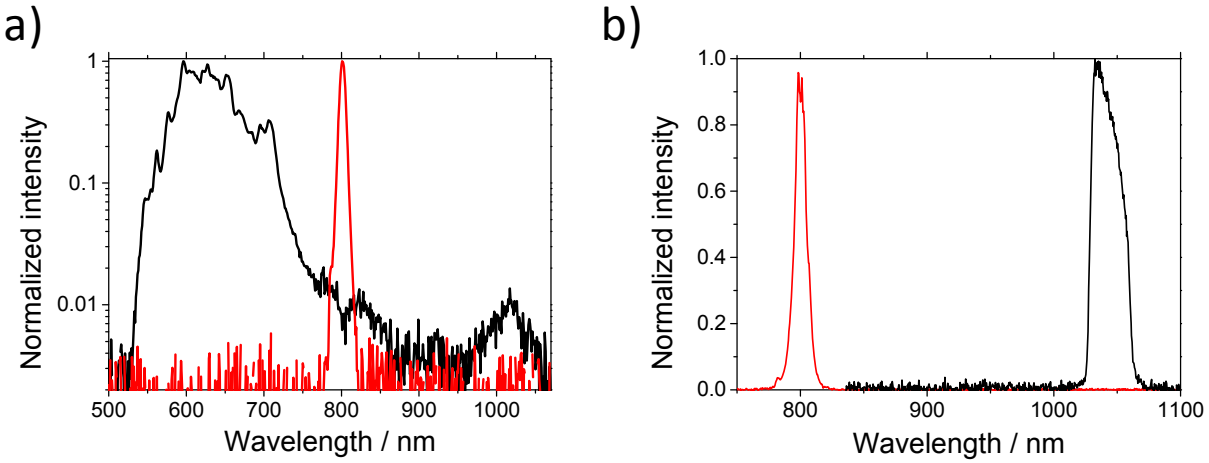

Fig. 2 a) Spectrum of 800-nm pulses (red line) and spectrum after spectral broadening by the PCF inside the WEU. b) Spectra of excitation pulses used for lipid CARS imaging: 800-nm pulses CARS pump/probe pulses and suitable part of the broadened spectrum from a around 1045 nm for the CARS-Stokes pulses.

Both excitation pulse trains were collinearly fed into the DermaInspect. Careful beam shaping was employed with a tunable telescope to further optimize the spatial overlap of CARS-Stokes and pump beams inside the focal volume. The temporal delay was set such that both pulse trains temporally overlapped at the sample position. This was verified by maximizing sum frequency generation and/or a lipid CARS signal from test samples. The power of CARS-Stokes and pump-pulse trains at the sample was typically a few mW and a few tens of mW and was for different skin depths.

Signals were collected by a two-channel detector (R9880U-20 and 1924A, Hamamatsu). CARS and TPF/SHG signals were spectrally separated by appropriate beam splitters and detected separately detected in the two channels ("CARS channel" and "TPF/SHG channel"). A further spectral separation of the TPF and SHG signals could be easily applied but has not been realized for measurements described here.

A shortpass filter (720 SP) was used to suppress residual laser light in front of dichroic mirror which split the CARS and TPF/SHG signals into the two channels. A narrow bandpass filter (Brightline BP 650-13) was placed inside the "CARS channel" to further suppress residual light. In the "TPF/SHG-channel" residual CARS signals were suppressed by a 600-nm short pass filter. The typical imaging time was 7.4 s/frame for images with 512 x 512 pixels. No further averaging was performed in order to reduce the measurement time and minimize movement artifacts. The CARS images typically had a maximum field of view of 200 x 200 μm^2. To record spectra, the two-channel detector was removed and fiber-coupling module was placed into the signal-beam path with only the 680-nm-short-pass filter in place. Spectra were recorded with a fiber-coupled thermo-electrically cooled CCD spectrometer (B&W Tek BTC112). The spectral data was

recorded while scanning for 30 s at a rate of 2 s/frame. The spectra represent the overall detected signals from the imaged regions without further corrections for the spectral sensitivity of the spectrometer and transmission of the system.

In vivo imaging was typically performed on the forearms of male and female volunteers and patients. A taped-fixed magnetic ring was used to ensure a fixed position of the focusing optics relative to the skin as described in Ref. 15. The measurements were performed at the Charité hospital in Berlin, Germany. All patients were informed about the procedure and risks and gave their written informed consent. The ethical guidelines of the Helsinki Declaration in biomedical research were followed. The measurements were further approved by an appropriate institutional review board.

3. RESULTS AND DISCUSSION

In vivo imaging has been performed on healthy skin of human volunteers. An example image is shown in Fig. 3. The Figure depicts a layer ("optical biopsy") perpendicular to the optical axes which lies about 24 µm below the skin surface. Fig. 3 a) shows cells with a typical round structure and dark cell nuclei. The inter-cell fluorescence mainly results from NAD(P)H[15]. The cell nuclei appear dark due to a lack of fluorescent material. Fig. 3 b) shows the corresponding image from the CARS channel which images CH_2 vibrational resonances at 2845 cm^{-1}. In Fig. 3 b) some cellular structures are also discernible. In addition, a cloud-like distribution of bright and dark areas is visible. This brightness distribution reflects the density of CH_2 containing molecules, i.e. in this layer most probably lipids.

Figure 4 shows images of the skin surface (stratum corneum) from the TPF/SHG and CARS channel, respectively. A round, curl-like structure indicates the end point of a sweat gland (indicated by an arrow in Fig. 4 a). The vertical black stripe in Fig. a) and b) which is visible from top to bottom of the images results from a gap in the skin surface, i.e. a microscopic wrinkle. In the image from the TPF/SHG channel (Fig. 4 a), flat, non-living cornified cells (corneocytes) are visible. The main fluorophore whose excitation leads to the image contrast is keratin. The CARS channel image (Fig. 4 b) shows similar corneocyte structures. This indicates a similar distribution of CH_2 containing molecules, in particular the keratin itself. Keratin is known to exhibit a strong CH_2-Raman peak at 2845 cm^{-1} [18].

The same skin area containing a part of a sweat gland as in Fig. 4 is also shown in Fig. 5 but recorded at a depth of about 18 µm below the skin surface. Fig. 5 a) and b) show images from TPF/SHG and CARS channel, respectively. The skin in this layer (stratum spinosum) hardly contains keratin. Here, cells around the region containing the sweat gland are visible in Fig. 5 a) and a fog-like intensity distribution appears in Fig. 5 b) resulting from CH_2 containing molecules, probably lipids. Fig. 5 c) and d) illustrate the effect of the temporal delay on the signals. Without temporal overlap between the CARS excitation pulses (i.e. pump/probe and Stokes pulses) the CARS signal vanishes (Fig. 5 d) except for residual autofluorescence at the center of the image which leaks into the CARS channel. The image from the TPF/SHG channel is not affected by the temporal delay (compare Fig. 5 c) and d) except by slight changes due to motion artifacts.

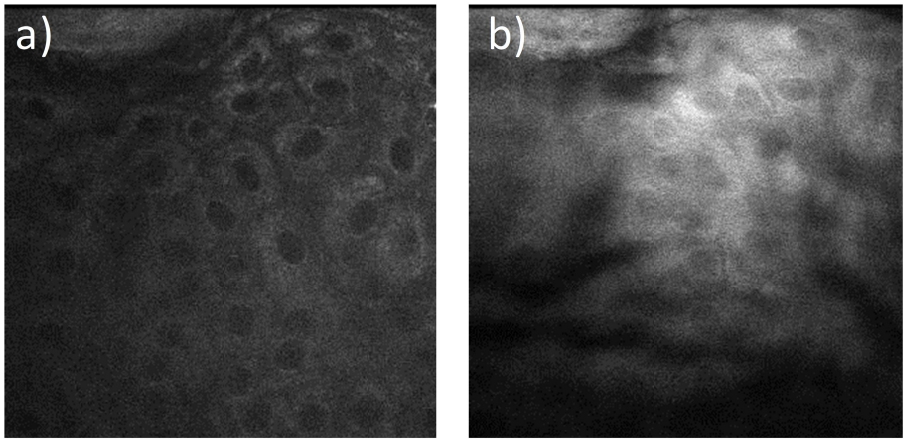

Fig. 3 In vivo multiphoton imaging of healthy human skin in vivo at a depth of about 24 µm. a) TPF/SHG channel, b) CARS channel. Each image depicts an area of 124 x 124 $µm^2$.

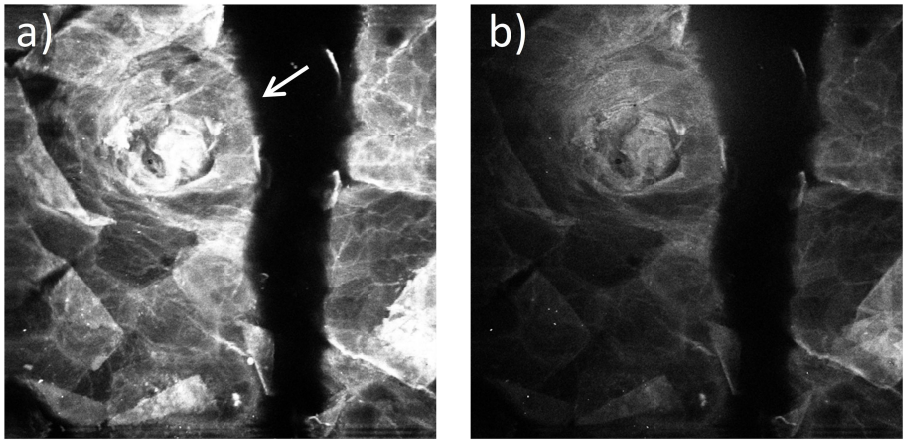

Fig. 4 In vivo multiphoton at the surface of healthy human skin in vivo. a) TPF/SHG-channel image, b) CARS-channel image. The arrow points to the ending point of a sweat gland. The dark vertical stripe indicates a microscopic skin wrinkle. Each image depicts an area of 190 x 190 µm2.

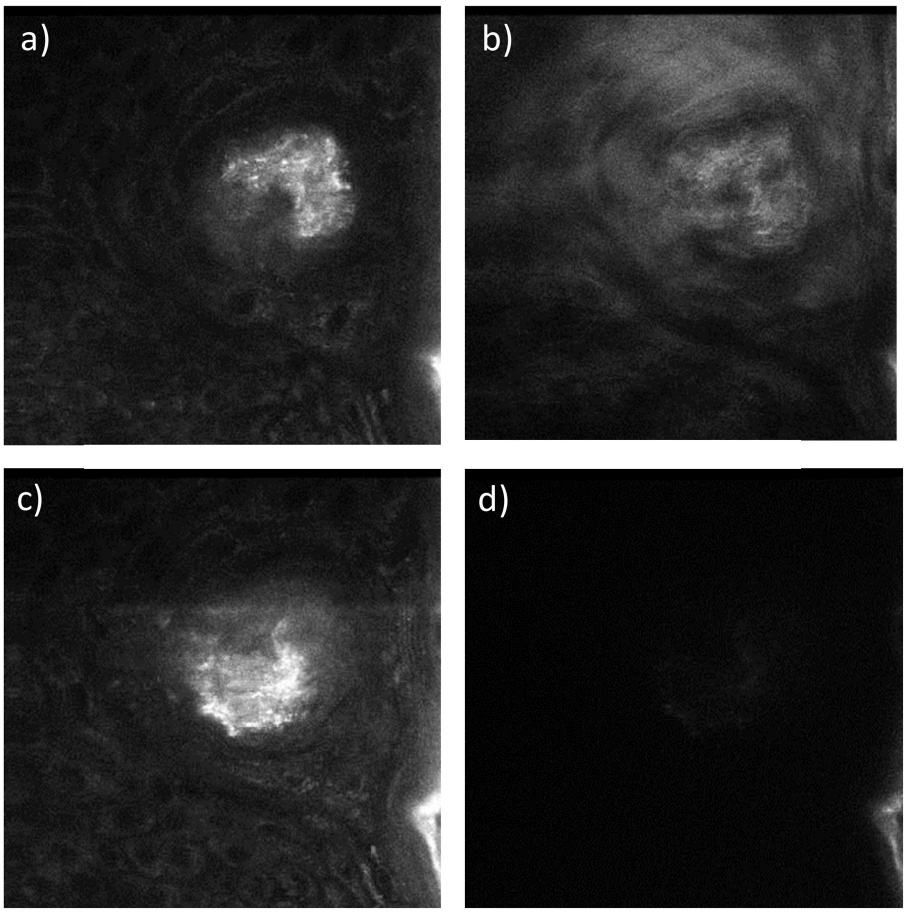

Fig. 5 In vivo multiphoton imaging of a sweat gland of healthy human skin in vivo about 18 µm bellow the skin surface. a) TPF/SHG-channel signal with temporal overlap of CARS-pump and Stokes pulses. b) CARS-channel signal with temporal overlap of CARS-pump and Stokes pulses. c) TPF/SHG-channel signal without temporal overlap of CARS-pump and Stokes pulses. d) CARS-channel signal without temporal overlap of CARS-pump and Stokes pulses. Each image depicts an area of 124 x 124 μm^2.

An example for imaging of a deeper laying layer (about 40 µm) is shown in Fig. 6. The Figure depicts a section from the stratum papillare which is known to contain SHG-generating collagen structures. The collagen SHG signals are visible and dominate in the TPF/SHG channel (Fig. 6 a). The CARS channel image in Fig. 6 b) shows a different intensity distribution. As can be seen the intensity distribution does follows the collagen structure visible in Fig. 6 a) but appears to be distributed over the whole imaged area. Although there are reports in the literature of CARS signals at 2845 cm^{-1} from collagen and elastin structures (for example in arterial tissues[14]), in Fig. 6 b) other molecules than collagen and elastin, dominate the image contrast, i.e. in this case probably lipid molecules.

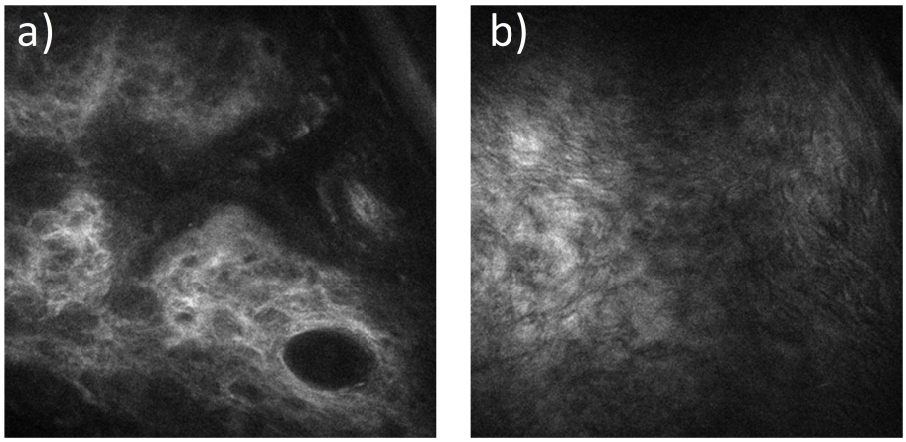

Fig. 6 In vivo multiphoton imaging of the human skin about 40 µm below the skin surface (stratum papillare). a) TPF/SHG-channel signal. b) CARS-channel signal. Each image depicts an area of 153 x 153 μm^2.

Further studies to collect reference CARS data from many individuals including persons who suffer from skin cancer and other skin diseases are currently in progress and will be subject of future publications.

4. CONCLUSION

A clinical CARS/TPF/SHG-multiphoton imaging system has been presented for in vivo imaging of human skin. The CARS excitation was realized by a two-beam setup. Fs pulses from a Ti:sapphire laser acted as CARS pump/probe pulses. The CARS-Stokes pulses were generated by spectrally broadening of the fs pulses in a PCF. Out of the resulting continuum spectrum a suitable part was selected by a band pass filter. Imaging was simultaneously performed in spectrally distinct CARS and TPF/SHG channels. Imaging examples of healthy human skin from different depths were presented and discussed. The images from the skin surface (stratum corneum) were similar in both channels due to keratin which is both fluorescent and Raman-active at 2845 cm^{-1}. Different fluorophore and CH_2-molecular distributions were found at layers deeper inside the skin which contained living cellular structures and/or elastin-collagen networks.

Acknowledgement
The support from Newport-Spectra Physics for loan of the MaiTai HP and in particular R. Zadoyan and his team to setup the WEU is thankfully acknowledged. The work was supported by German Federal Ministry of Education and Research (BMBF) under the national project (BMBF project Chemoprävent - Development of prevention strategies against dermal side-effects of chemotherapy, project number 13N10507).

References

[1] Zipfel, W. R., Williams, R. M., and Webb, W. W., "Nonlinear magic: multiphoton microscopy in the biosciences," Nat Biotechnol 21 (11), 1369-1377 (2003).

[2] Pezacki, J. P., Blake, J. A., Danielson, D. C., Kennedy, D. C., Lyn, R. K., and Singaravelu, R., "Chemical contrast for imaging living systems: molecular vibrations drive CARS microscopy," Nat Chem Biol 7 (3), 137-145 (2011).

[3] Zumbusch, A., Holtom, G. R., and Xie, X. S., "Three-Dimensional Vibrational Imaging by Coherent Anti-Stokes Raman Scattering," Physical Review Letters 82 (20), 4142 (1999).
[4] König, K., Breunig, H. G., Bückle, R., Kellner-Höfer, M., Weinigel, M., Büttner, J., Sterry, W., and Lademann, J., "Optical skin biopsies by clinical CARS and multiphoton fluorescence/SHG tomography," Laser Physics Letters 8 (6), 4 (2011).
[5] Breunig, H. G., Bückle, R., Kellner-Höfer, M., Weinigel, M., Lademann, J., Sterry, W., and König, K., "Combined in vivo multiphoton and CARS imaging of healthy and disease-affected human skin," Microsc Res Tech 75 (4), 492-498 (2012).
[6] Breunig, H. G., Weinigel, M., Bückle, R., Kellner-Höfer, M., Lademann, J., Darvin, M. E., W.Sterry, and König, K., "Clinical coherent anti-Stokes Raman scattering and multiphoton tomography of human skin with a femtosecond laser and photonic crystal fiber," Laser Physics Letters 10, 025604 (2013).
[7] König, K., "Clinical multiphoton tomography," J Biophotonics 1 (1), 13-23 (2008).
[8] König, K., Raphael, A. P., Lin, L., Grice, J. E., Soyer, H. P., Breunig, H. G., Roberts, M. S., and Prow, T. W., "Applications of multiphoton tomographs and femtosecond laser nanoprocessing microscopes in drug delivery research," Adv Drug Deliv Rev 63 (4-5), 388-404 (2011).
[9] Zipfel, W. R., Williams, R. M., Christie, R., Nikitin, A. Y., Hyman, B. T., and Webb, W. W., "Live tissue intrinsic emission microscopy using multiphoton-excited native fluorescence and second harmonic generation," PNAS 100 (12), 7075-7080 (2003).
[10] Evans, C. L. and Xie, X. S., "Coherent anti-stokes Raman scattering microscopy: chemical imaging for biology and medicine," Annu Rev Anal Chem 1, 883-909 (2008).
[11] Suhalim, J. L., Boik, J. C., Tromberg, B. J., and Potma, E. O., "The need for speed," J Biophotonics 5 (5-6), 387-395 (2012).
[12] Cheng, J.-X. and Xie, X. S., "Coherent Anti-Stokes Raman Scattering Microscopy: Instrumentation, Theory, and Applications," J Phys Chem B 108 (3), 827-840 (2003).
[13] Chen, B. C., Sung, J., Wu, X., and Lim, S. H., "Chemical imaging and microspectroscopy with spectral focusing coherent anti-Stokes Raman scattering," J Biomed Opt 16 (2), 021112 (2011).
[14] Wang, H. W., Le, T. T., and Cheng, J. X., "Label-free Imaging of Arterial Cells and Extracellular Matrix Using a Multimodal CARS Microscope," Opt Commun 281 (7), 1813-1822 (2008).
[15] Breunig, H. G., Studier, H., and König, K., "Multiphoton excitation characteristics of cellular fluorophores of human skin in vivo," Opt Express 18 (8), 7857-7871 (2010).
[16] Zadoyan, R., Baldacchini, T., Carter, J., C.-H., K., and Ocepek, D., "CARS module for multimodal microscopy," Proc. of SPIE 7903, 79039Z-79031-79039 (2011).
[17] Fischer, F., Volkmer, B., Puschmann, S., Greinert, R., Breitbart, W., Kiefer, J., and Wepf, R., "Risk estimation of skin damage due to ultrashort pulsed, focused near-infrared laser irradiation at 800 nm," J Biomed Opt 13 (4), 041320 (2008).
[18] Edwards, H. G., Hunt, D. E., and Sibley, M. G., "FT-Raman spectroscopic study of keratotic materials: horn, hoof and tortoiseshell," Spectrochim Acta A Mol Biomol Spectrosc 54A (5), 745-757 (1998).